

Organofluoro-silica xerogels as high-performance optical oxygen sensors

Rosaria Ciriminna and Mario Pagliaro*

First published as an Advance Article on the web 9th June 2009

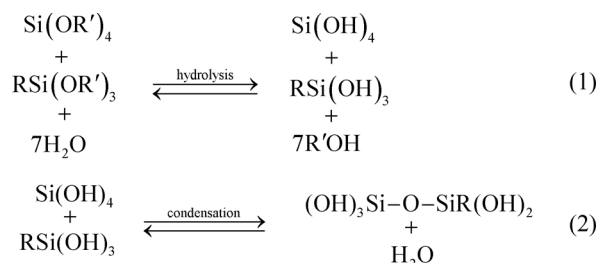
DOI: 10.1039/b819417c

Ubiquitous oxygen (O₂) is one of the most important analytes to be assessed in medicine, industry and the environment. Due to a number of advantages, miniaturized optical sol–gel sensors are rapidly replacing older electrochemical sensors. This account provides an overview of fluorinated organically modified silicate (ORMOSIL) xerogels as optical chemical sensors and shows how, together with the dye quenching rate, the subtle structural features of an organofluoro-silica matrix is of fundamental importance in determining the overall sensor performance.

1. Background and introduction

Doped sol–gel silicas are well established platforms for optical sensors due to their high transparency and high sensitivity to external reactants, coupled with unsurpassed versatility and stability.¹ Oxygen, in its turn, is perhaps the single most important analyte in analytical chemistry. O₂ is involved in many chemical and biochemical conversions as either a reactant or a product and its concentration often needs to be measured in medicine, industry and the environment. The search for optical O₂ sensors to replace the conventional electrochemical (Clarke) electrodes has been a major goal of recent chemical research, with studies focusing on polymers² and on sol–gel silicas.³

Optical oxygen sensors are more attractive than conventional amperometric devices because they have a fast response time, do not consume oxygen, are highly stable and do not require frequent calibration. Organically modified silicates (ORMOSILs)⁴ are easily prepared by mild co-condensation of silicon alkoxides functionalized with stable non-hydrolysable organic groups, in the presence of the photoactive species.⁵ The mechanism involves hydrolysis and condensation reactions (eqn (1) and



Scheme 1 The sol–gel hydrolytic polycondensation affording ORMOSILs.

(2) in Scheme 1), and in analytical applications the intermediate gels are generally shaped as thin-films or microfibers:⁶

The overall hydrolytic polycondensation reaction can be written as eqn (3):



The chemical and physical properties of the final doped glasses (porosity, surface area, pore size distribution, shape, hydrophilic–lipophilic balance *etc.*) can be finely tuned in an immense range by selecting appropriate sol–gel process conditions. The advantages offered by these materials over traditional commercial electrochemical sensors are well rendered by the comparison

Istituto per lo Studio dei Materiali Nanostrutturati, CNR, via Ugo La Malfa 153, 90146 Palermo, Italy. E-mail: rosaria.ciriminna@ismn.cnr.it; mario.pagliaro@ismn.cnr.it



Rosaria Ciriminna

Rosaria Ciriminna (1971) is a research chemist at Italy's CNR Institute of Nanostructured Materials. Rosaria's interest in organic and materials chemistry spans from catalysis for fine chemicals to sensing, functional coatings and photovoltaics. She has co-authored 3 books, 4 patents and some 70 research papers.



Mario Pagliaro

Mario Pagliaro (1969) is a scholar in chemistry and management based at Palermo's CNR. His research and educational interests in chemistry, materials science and science methodology are documented in 8 books, 5 patents and some 80 research papers. Often cited for his excellence in teaching, Mario leads Sicily's Photovoltaics Research Pole and currently chairs the organization of the FIGIPAS 2009 conference.

Table 1 Advantages of optical O₂ sensors over traditional commercial electrochemical sensors (adapted from OceanOptics.com)

Fiber-optic oxygen sensors	Commercial electrochemical systems
Based on dynamic equilibrium with surrounding media, O ₂ is not consumed	Measure the rate of consumption of O ₂
Responds to pO ₂ ; calibration is the same in both gases and liquids	Electrodes can be calibrated for use in gases or liquids, but not both at the same time
Immune to sample matrix, salinity and pH	Affected by the sample matrix; changes in salinity, pH affects sensor readings
Fast response times: <1 s for dissolved O ₂ and O ₂ gas	Response times of 60–90 s
Long life (>1 year)	Electrode lifetime <3 months
Frequent calibration unnecessary	Calibration may be required on an hourly basis
Probe temperature range –80 to 80 °C	Temperature range 0 to 45 °C

**Fig. 1** The “RedEye” oxygen optical sensor for non-invasive O₂ detection enables quick readings of the presence or absence of oxygen, and provides quantitative measurements. (Photo courtesy of Ocean Optics, Inc.)

between a fiber-optic doped xerogel O₂ sensor and the older Clarke electrode (Table 1).

One such sol–gel commercial sensor (made of propyl-modified silica) used to measure oxygen levels in packaging and other enclosed containers in medical, pharmaceutical, food and beverage applications is available from US-based company Ocean Optics.⁷

The patch (Fig. 1) can be integrated into the surface of sample containers such as blood bags, pill blister packs, or point-of-care analysis devices, to permit non-invasive, through-the-package oxygen concentration measurements. Such optical sensors are capable of monitoring low levels of oxygen in gases (to 0.005%) and dissolved oxygen in liquids (to 20 ppb), as well as the higher oxygen levels present in cell culture and respiratory monitoring.

These optical sensors are based on fluorescence or phosphorescence quenching of the radiation emitted by a photoactive sol–gel entrapped dopant by the analyte molecule. O₂ access to the entrapped sensitizer causes a reduction of dye luminescence intensity that can be directly correlated to the analyte concentration. For example, O₂-responsive sensor arrays and films formed by sequestering the ruthenium-based sensitizer tris(4,7-diphenyl-1,10-phenanthroline)ruthenium(II) [Ru(dpp)₃]²⁺ within

ORMOSIL hybrid xerogels are among the best platforms for oxygen sensing⁸ thanks to their excellent permeability to oxygen (which enables fast response), high sensitivity (20 ppb) detection limit due to long excited lifetime (5.3 μs), high luminescence quantum yield and O₂ quenching efficiency. The sensitivity of the sensor, in fact, depends both on the rate of luminophore quenching by O₂, the permeability of the solid matrix to O₂, and on the accessibility of the entrapped luminophore. Assuming that the ensemble of luminophore molecules are emitted from largely similar microenvironments, and that the quencher molecules have similar accessibilities to the individual luminophore molecules, one can write the Stern–Volmer relationship (eqn 4):⁹

$$I_0/I = 1 + K_{SV}[O_2] = 1 + k_q\tau_0[O_2] \quad (4)$$

where I_0 and I represent the intensities of luminescence in the absence and presence of O₂, respectively, K_{SV} is the Stern–Volmer quenching constant, $[O_2]$ is the O₂ concentration, τ_0 is the excited-state luminescence lifetime in the absence of quencher, and k_q is the bimolecular rate constant describing the efficiency of the collisional encounters between the luminophore and the quencher.

For the ideal case of a luminophore in a homogeneous microenvironment, a plot of I_0/I vs. $[O_2]$ will be linear with a slope equal to K_{SV} and an intercept of unity, allowing a simple single-point calibration of the sensor. On the other hand, a downward-curving Stern–Volmer plot is due to the presence of a multitude of quenching sites within the sensing element, each site with its own Stern–Volmer constant. Sensitivity is measured by the ratio I_{N_2}/I_{O_2} , where I_{N_2} and I_{O_2} represent the fluorescence intensities in pure nitrogen and pure oxygen environments, respectively (a large ratio pointing to an increase in K_{SV}).

2 Enhanced performance of fluorinated composites

In general, fluorinated precursors mixed with alkyl-modified silanes form uniform, crack-free xerogel films that can be used to construct O₂ sensors that have linear calibration curves, have excellent long-term stability and afford unprecedented sensitivity. Following the first such sensor based on [Ru(dpp)₃]²⁺ entrapped in an *n*-propyl-trimethoxysilane/3,3,3-trifluoropropyl-trimethoxysilane (C3-TMOS/TFP-TMOS),¹⁰ showing a then unprecedented I_{N_2}/I_{O_2} sensitivity of 35 and a response time of less than 5 s, other composite sensors (made of two of the following silanes: tetramethoxysilane (TMOS), *n*-propyl-trimethoxysilane (C3-TMOS), 3,3,3-trifluoropropyl-trimethoxysilane (TFP-TMOS), phenethyl-trimethoxysilane (PE-TMOS), and pentafluorophenylpropyl-trimethoxysilane (PFP-TMOS) were studied in detail (Fig. 2).¹¹

Most recently even more sensitive high performance fiber-optic O₂ sensors based on fluorinated xerogels doped with Pt(II) complexes were reported.¹² A general result of these studies is that encapsulation of the luminophore within fluorinated silica composites, instead of simple alkyl-modified analogues, enhances the overall performance of the optical sensors.

Representative examples for [Ru(dpp)₃]²⁺-based quenchometric sensors are listed in Table 2, where the sensitivity of several fluorinated sensors is reported (with the molar ratio F/N of fluorinated to non-fluorinated precursors set at 2).

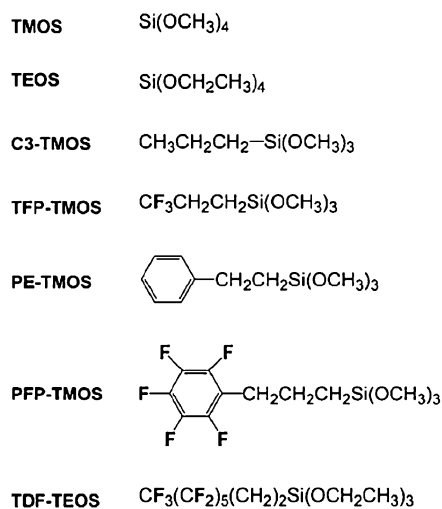


Fig. 2 Chemical structures of the silane precursors used in Bright and co-workers' comparative study. (Reproduced with permission from ref. 11. Copyright 2006, Society for Applied Spectroscopy.)

First generation fluorinated sensors were made of $[\text{Ru}(\text{dpp})_3]^{2+}$ doped in a TFP-TMOS/C3-TMOS matrix with $F/N = 2$, and exhibited an $I_{\text{N}_2}/I_{\text{O}_2}$ of 35 ± 4 ; at that time a sensitivity significantly greater than observed with any previous $[\text{Ru}(\text{dpp})_3]^{2+}$ -based quenchometric sensor, with a fast 5 s response time when switching from a fully deoxygenated environment to a fully oxygenated environment. Furthermore, the Stern–Volmer plot is linear over the full oxygen concentration range (0–100%), indicating that the $[\text{Ru}(\text{dpp})_3]^{2+}$ molecules are reporting from a *homogeneous* microenvironment, since in any case the non-linearity is associated with the luminophore dopant molecules distributed between different sites that exhibit different k_q or τ_0 values, as is often the case with many other xerogel-based sensor platforms that exhibit downward curvature and multi-exponential time-resolved intensity decay profiles.

In general, however, entrapment of the Ru-based luminophore in the other xerogels studied in the elegant comparative study

mentioned above,¹⁰ was not homogeneous with the time-resolved intensity decay profiles of the luminescence due to the entrapped $[\text{Ru}(\text{dpp})_3]^{2+}$ being well described by the Lehrer model consistent with the $[\text{Ru}(\text{dpp})_3]^{2+}$ molecules reporting from two microenvironments within the xerogel matrix, one of which is accessible to, and responsive to, the O_2 quencher molecules, and one in which the luminophore is not accessible to or is non-responsive to the quencher molecules.¹⁰

Results in particular showed that while the observed $I_{\text{N}_2}/I_{\text{O}_2}$ for the TFP-TMOS/C3-TMOS hybrid xerogel with the molar ratio $F/N = 1$ is the best among $[\text{Ru}(\text{dpp})_3]^{2+}$ -based O_2 -responsive sensor elements, the sensitivity to O_2 could be adjusted by more than 25-fold by controlling the F/N parameter. In detail, the k_q for the TFP-TMOS/C3-TMOS xerogel was the largest among all materials studied reaching a maximum around $F/N = 0.5$ and dropping by 30–50% as one moves away from the optimal F/N (Fig. 3).

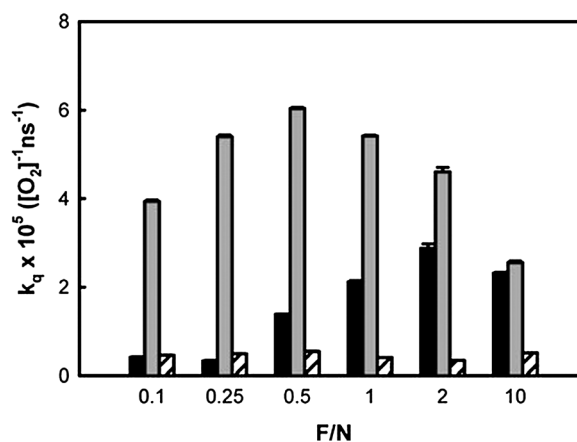


Fig. 3 Effects of the molar ratio of fluorinated and non-fluorinated siloxane precursor (F/N) on the bimolecular quenching constant (k_q) for the TFP-TMOS/C3-TMOS xerogels, shown by grey bars. Black and white bars refer to hybrid xerogels obtained from TFP-TMOS/TMOS and TFP-TMOS/PE-TMOS, respectively (reprinted with permission from ref. 11. Copyright 2006, Society for Applied Spectroscopy.)

Table 2 Representative examples of reported $I_{\text{N}_2}/I_{\text{O}_2}$ for quenchometric oxygen sensors based on dyes immobilized in sol-gel matrixes (adapted with permission from ref. 10; Copyright 2005, ACS Publications)

O_2 -sensitive dye	Support matrix	Response time	$I_{\text{N}_2}/I_{\text{O}_2}$	Ref.
$[\text{Ru}(\text{dpp})_3]^{2+}$	TEOS ^a	0% O_2 to 100% O_2 : 3.5 s; 100% O_2 to 0% O_2 : 30 s	12	13
$[\text{Ru}(\text{dpp})_3]^{2+}$	MeTMOS	10 s	3.4	8
$[\text{Ru}(\text{dpp})_3]^{2+}$	C8-TEOS ^b /TEOS	None	16.48	3
$[\text{Ru}(\text{dpp})_3]^{2+}$	C3-TMOS/TFP-TMOS	Sensors response times were <5 s	35	10
PtOEP ^c	TEOS	60–540 s for the changes for different oxygen concentration	40	14
PtTFPP ^c	C8-TEOS/TEOS	0% O_2 to 100% O_2 : 0.6 s; 100% O_2 to 0% O_2 : 5 s	22	15
PtOEP	C8-TEOS/TEOS	0% O_2 to 100% O_2 : 0.7 s; 100% O_2 to 0% O_2 : 14 s	47	14
PtTFPP	C3-TMOS/TFP-TMOS	0% O_2 to 100% O_2 : 3.7 s; 100% O_2 to 0% O_2 : 5.3 s	68.7	12
PtOEP	C3-TMOS/TFP-TMOS	0% O_2 to 100% O_2 : 3.7 s; 100% O_2 to 0% O_2 : 5.9 s	82.5	12

^a TEOS = tetraethoxysilane. ^b C8-TEOS = *n*-octyl-triethoxysilane. ^c PtOEP = Pt(II) octaethylporphine; PtTFPP = Pt(II) tetrakis pentafluorophenylporphine.

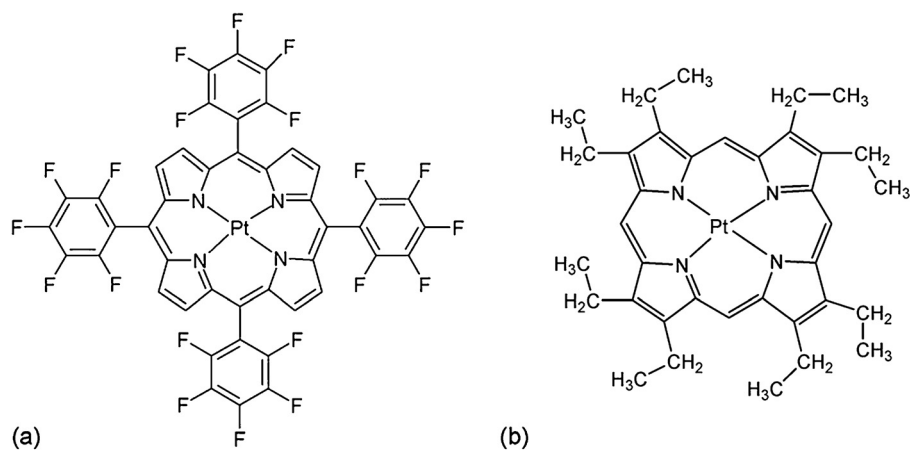


Fig. 4 Chemical structures of: (a) PtTFPP and (b) PtOEP complexes.

Thus, the reason for the observed sensitivity from these xerogel-based materials arises from k_q and τ_0 both being larger in comparison to the other systems studied; however, the tunability arises exclusively from k_q and not from τ_0 .

From a morphological viewpoint, the smoothness and the homogeneity of the composite ORMOSIL films is very high and their crack-free formation proceeded without any added surfactant, due to enhanced hydrophobicity and consequent lower surface tension at the solid/liquid interface during drying of the intermediate alcogel. Under ambient storage conditions, the stability of these hybrid xerogel sensors was constant to within 2% over a six-month period which should be compared to the 5-fold decrease in sensitivity in pure TEOS-based xerogels. Such a stable sensor response over time is due to the increased hydrophobicity of the sol-gel ORMOSIL cages that overcomes the xerogel shrinkage and pore collapse with time, and is a crucial factor in the development of a reliable sensor platform. This outcome, in particular, contrasts with the poor stability of most sensing species immobilized at the surface of organic and inorganic polymers.¹⁶

Based on these findings, more recently two innovative phosphorescent Pt porphyrins (Fig. 4) entrapped in the same organofluoro-silica glass TFP-TMOS/C3-TMOS were used to construct the most sensitive optical oxygen sensors known thus far. Produced as optical fibers, such sensors employ either Pt(II) tetrakis pentafluorophenylporphine (PtTFPP) or Pt(II) octaethylporphine (PtOEP). These platinum species have longer lifetimes than Ru(II) dyes, show convenient excitation and emission wavelengths with large Stokes shifts (100–170 nm), and also have a lower luminescence quantum yield. As a result, the optical O₂ sensors based on composite fluoro-xerogels doped with PtTFPP or PtOEP luminophores have sensitivities of 68.7 and 82.5, respectively, both yielding linear Stern–Volmer plots (Fig. 5).

Again, the excellent sensitivity of these sensors was attributed to the uniform distribution of the Pt(II) luminophores in the xerogel matrix, and to the improved oxygen diffusivity provided by the fluorinated xerogel. Furthermore, longer excitation and

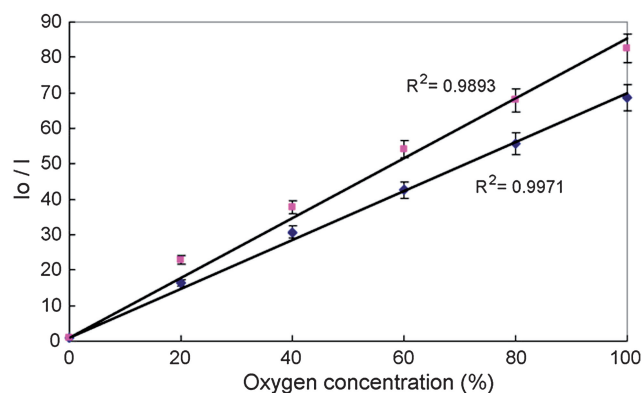


Fig. 5 Stern–Volmer plots for PtTFPP-doped (◆) and PtOEP-doped (■) oxygen sensors. (Reprinted with permission from ref. 12. Copyright 2007, Elsevier.)

emission wavelengths increase the signal-to-background noise ratio of oxygen sensors, which is particularly useful for *in vivo* measurements.

The response time of the PtTFPP-doped sensor is 3.7 s when switching from 100% nitrogen to a fully oxygenated environment, and 5.3 s when switching the opposite way (the corresponding response times of the PtOEP-doped sensor are 3.7 and 5.9 s, respectively), Fig. 6. Longer reaction times are, of course, to be expected on changing from 100% nitrogen to atmospheric oxygen concentration.

The approach using organofluoro-alkoxides has a broad applicability and was extended by Chu and Lo to the production of a fiber-optic CO₂ sensor.¹⁷ The fluorinated platform exhibited a linear response to CO₂ concentrations in a wide concentration range (0–30%) whereas in previously reported pyranine-based sensors using alkyl-modified silicon alkoxide, the linear response was limited to 2% CO₂.¹⁸

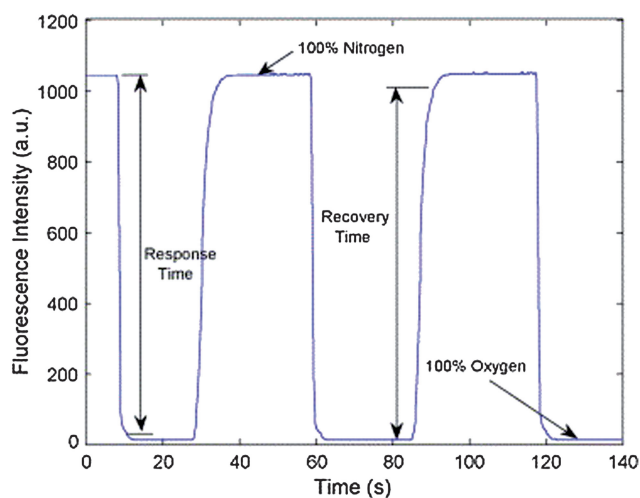


Fig. 6 Response time and fluorescence intensity change of PtTFPP-doped sensor when switching between 100% nitrogen and 100% oxygen. (Reprinted with permission from ref. 12. Copyright 2007, Elsevier.)

3 Outlook and conclusions

Fluorinated ORMOSILs doped with sensitizing luminophores provide appropriate sensing films for oxygen sensors thanks to (i) the homogeneous fluorinated microenvironment of the sol-gel cages entrapping the luminophore species, and to (ii) the exceptional diffusivity of the O₂ molecules within the fluorine-modified matrix. As a result, highly sensitive sensors can be obtained with a rapid detection time, linear calibration and stable performance. Pt porphyrins are the best suited sensing species affording the highest O₂ sensitivity and response rapidity of any reported dye-based sensor platform (68.7 and 82.5 sensitivities for the PtTFPP-doped and PtOEP-doped sensors, respectively; and 4–5 s response times). Ruthenium species such as [Ru(dpp)₃]²⁺ also exhibit excellent performance (35 sensitivity and *ca.* 5 s response times).

Attentive readers may have noted that partial fluorination of the organosilica matrix ($F/N = 1$ for the [Ru(dpp)₃]²⁺-based sensors) affords the most sensitive sensors. Indeed, a remarkable correlation between the hydrophilic–hydrophobic balance (HHB) of the matrix and reactivity has recently been found to explain the high performance of similarly doped fluorinated xerogels in aerobic catalysis.¹⁹ The HHB depends on the degree of fluorination and on the length of the fluoroalkyl chain linked to the silica network, and reaches a maximum for low $F=N$ values. An insight that will be useful in developing second

generation sol-gel entrapped fluorinated silicas for sensing and catalytic applications alike.

The use of a hybrid xerogel support matrix has a number of key advantages compared to previously reported surface-functionalized polymers, including good photostability and high sensitivity to the external environment. Furthermore, the hybrid xerogel matrix provides a simple solution for the production of robust, hydrophobic thin-films with well-defined thickness and excellent gas permeability characteristics for use in planar waveguide fluorescence detection configurations. Considering the ease of miniaturization and fabrication of these sol-gel derived sensors, the introduction of commercial fluorinated sol-gel derived O₂ and CO₂ sensors is only a matter of time.

Acknowledgements

This article is dedicated to University of New York at Buffalo's Frank V. Bright for his magnificent contributions to the development of sol-gel optical sensors, and for many years of fruitful collaboration.

References

- 1 C. McDonagh, C. S. Burke and B. D. McCraith, *Chem. Rev.*, 2008, **108**, 400.
- 2 Y. Amao, *Microchim. Acta*, 2003, **143**, 1.
- 3 Y. Tang, E. C. Tehan, Z. Tao and F. V. Bright, *Anal. Chem.*, 2003, **75**, 2407.
- 4 O. Lev, M. Tsionsky, L. Rabinovich, V. Glezer, S. Sampath and I. Pankratov, *Anal. Chem.*, 1995, **67**, 22A.
- 5 M. Pagliaro, R. Ciriminna, M. Wong Chi Man and S. Campestri, *J. Phys. Chem. B*, 2006, **110**, 1976.
- 6 M. Pagliaro, *Silica-Based Materials for Advanced Chemical Applications*, RSC Publishing, Cambridge, 2009.
- 7 See also at the URL: www.oceanoptics.com.
- 8 C. McDonagh, B. D. McCraith and A. K. McEcoy, *Anal. Chem.*, 1998, **70**, 45.
- 9 J. R. Lackowicz, *Principles of Fluorescence Spectroscopy*, Kluwer Academic/Plenum Press, New York, 2nd edition, 1999, ch. 8 and 9.
- 10 R. M. Bukowsky, R. Ciriminna, M. Pagliaro and F. V. Bright, *Anal. Chem.*, 2005, **77**, 2670.
- 11 R. M. Bukowski, M. D. Davenport, A. H. Titus and F. V. Bright, *Appl. Spectrosc.*, 2006, **60**, 951.
- 12 C. S. Chu and Y. L. Lo, *Sens. Actuators, B*, 2007, **124**, 376.
- 13 A. N. Watkins, B. R. Wenner, J. D. Jordan, W. Y. Xu, J. N. Demas and F. V. Bright, *Appl. Spectrosc.*, 1998, **52**, 750.
- 14 S. K. Lee and I. Okura, *Anal. Chim. Acta*, 1997, **342**, 181.
- 15 S. Yeh, C. S. Chu and Y. L. Lo, *Sens. Actuators, B*, 2006, **119**, 701.
- 16 R. F. Taylor, *Protein Immobilization: Fundamental and Applications*, Marcel Dekker, New York, 1991, ch. 8.
- 17 C. S. Chu and Y. L. Lo, *Sens. Actuators, B*, 2008, **129**, 120.
- 18 C. Malins and B. D. McCraith, *Analyst*, 1998, **123**, 2373.
- 19 A. Fidalgo, R. Ciriminna, L. M. Ilharco, S. Campestri, M. Carraro and M. Pagliaro, *Phys. Chem. Chem. Phys.*, 2008, **10**, 2026.